

# Spin- $\frac{1}{2}$ Heisenberg ladder: variation of entanglement and fidelity measures close to quantum critical points

Amit Tribedi and Indrani Bose

September 2, 2021

Department of Physics

Bose Institute

93/1, Acharya Prafulla Chandra Road

Kolkata - 700 009, India

## Abstract

We consider a two-chain, spin- $\frac{1}{2}$  antiferromagnetic Heisenberg spin ladder in an external magnetic field  $H$ . The spin ladder is known to undergo second order quantum phase transitions (QPTs) at two critical values,  $H_{c1}$  and  $H_{c2}$ , of the magnetic field. There are now known examples of strongly coupled (rung exchange interaction much stronger than nearest-neighbour intrachain exchange interaction) organic ladder compounds in which QPTs have been experimentally observed. In this paper, we investigate whether well-known bipartite entanglement measures like one-site von Neumann entropy, two-site von Neumann entropy and concurrence develop special features close to the quantum critical points. As suggested by an earlier theorem, the first derivatives of the measures with respect to magnetic field are expected to diverge as  $H \rightarrow H_{c1}$  and  $H \rightarrow H_{c2}$ . Based on numerical diagonalization data and a mapping of the strongly-coupled ladder Hamiltonian onto the  $XXZ$  chain Hamiltonian, for which several analytical results are known, we find that the derivatives of the entanglement measures diverge as  $H \rightarrow H_{c2}$  but remain finite as  $H \rightarrow H_{c1}$ . The reason for this discrepancy is analysed. We further calculate two recently proposed quantum information theoretic measures, the reduced fidelity and reduced fidelity susceptibility, and show that these measures provide appropriate signatures of the QPTs occurring at the critical points  $H = H_{c1}$  and  $H = H_{c2}$ .

PACS number(s): 03.67.Mn

## I. INTRODUCTION

Antiferromagnetic (AFM) Heisenberg ladders are examples of interacting many body systems which exhibit a range of novel phenomena [1, 2]. An  $n$ -chain spin ladder consists of  $n$  chains coupled by rungs, the simplest example being a two-chain ladder with  $n = 2$ . The study of ladders as prototypical many body systems became important after the discovery of high temperature superconductivity in the strongly correlated cuprate materials. The dominant electronic and magnetic properties of

the cuprates are associated with the  $CuO_2$  planes which have the structure of a square lattice [3]. The level of rigour that can be achieved in the treatment of strong correlation is less in two dimensions (2d) than in 1d. Ladder models, with structure interpolating between 1d and 2d, serve as ideal candidates to address issues related to strong correlation and also to investigate how electronic and magnetic properties change as one progresses from the chain to the plane. In undoped ladder models, each site of the ladder is occupied by a spin (usually of magnitude  $\frac{1}{2}$ ) and the spins interact via the AFM Heisenberg exchange interaction. In doped ladder models, some of the spins are replaced by positively charged holes which are mobile. The Hamiltonian describing the doped systems are the t-J and Hubbard ladder models [1, 2, 3]. With the discovery of a large number of materials having a ladder-like structure, the study of ladders has acquired considerable importance. The materials exhibit a range of phenomena including superconductivity in hole-doped systems, the ‘odd-even’ effect in which the excitation spectrum of an  $n$ -chain ladder is gapped (gapless) if  $n$  is even (odd) and quantum phase transitions (QPTs) tuned by an external magnetic field [1, 2, 3]. Many of the experimental observations were motivated by theoretical predictions, superconductivity being a prime example [4, 5, 6].

In this paper, we focus on QPTs in a two-leg AFM Heisenberg ladder (Fig. 1) in an external magnetic field. The Hamiltonian describing the model is given by

$$\mathcal{H} = \sum_{j=1}^L [J_{\parallel}(\mathbf{S}_{1,j} \cdot \mathbf{S}_{1,j+1} + \mathbf{S}_{2,j} \cdot \mathbf{S}_{2,j+1}) + J_{\perp} \mathbf{S}_{1,j} \cdot \mathbf{S}_{2,j}] - H \sum_{j=1}^L (S_{1,j}^z + S_{2,j}^z) \quad (1)$$

where the indices 1 and 2 distinguish the lower and upper legs of the ladder and  $j$  labels the rungs. The spins have magnitude  $\frac{1}{2}$  ( $|\mathbf{S}_j| = \frac{1}{2}$ ) and interact via the AFM Heisenberg exchange interaction. The intrachain and rung exchange couplings are of strengths  $J_{\parallel}$  and  $J_{\perp}$  respectively. The total number of rungs is  $L$  and periodic boundary conditions are assumed. The factor  $g\mu_B$  ( $g$  is the Landé splitting factor and  $\mu_B$  the Bohr magneton) is absorbed in  $H$ . If  $J_{\perp} = 0$ , the ladder decouples into two non-interacting spin- $\frac{1}{2}$  Heisenberg chains with no gap to spin excitations. For any arbitrary  $J_{\perp} \neq 0$ , the excitation spectrum acquires a gap (spin gap). In the strong coupling limit,  $J_{\perp} \gg J_{\parallel}$ , a simple physical picture of the ground state and the origin of the spin gap can be given. The spins along the rungs predominantly form singlets in the ground state. A spin excitation is created by replacing a singlet by a triplet which propagates along the ladder due to the intrachain exchange interaction. In first order perturbation theory, the spin gap  $\Delta$  is given by  $\Delta \approx J_{\perp} - J_{\parallel}$  separating the lowest excited state from the dimerized ground state.

There are now several known strong coupling ladder compounds [7]. Of these, the organic ladder compounds  $Cu_2(C_5H_{12}N_2)_2Cl_4$  [8],  $(C_5H_{12}N)_2CuBr_4$  [9] and  $(5IAP)_2CuBr_4 \cdot 2H_2O$  [10] are of special interest because of the experimental observation of the QPTs in these systems by the tuning of an external magnetic field. A QPT occurs at  $T = 0$  and brings about a qualitative change in the ground state of an interacting many body system at a specific value  $g_c$  of the tuning parameter  $g$  [11]. QPTs are driven by quantum fluctuations and in the case of second order transitions, the quantum critical point is associated with scale invariance and a diverging correlation length. The ground state energy becomes non-analytic at the critical value  $g_c$  of the tuning parameter. If one of the phases is gapped, the gap goes to zero in a power-law fashion as  $g \rightarrow g_c$ . In the case of a spin ladder, the external magnetic field  $H$  plays the role of the tuning parameter  $g$ . There are two critical points,  $H_{c1}$  and  $H_{c2}$  [7, 8, 9, 10]. At  $T = 0$  and for  $0 < H < H_{c1}$ , the ladder is in the spin gap phase. In the presence of the magnetic field, there is a Zeeman splitting of the triplet ( $S = 1$ ) excitation spectrum with the  $S^z = 1$  component having the lowest energy. The spin gap

is now  $\Delta - H$ . At  $H = H_{c1} = \Delta$ , the gap closes and a QPT occurs to the Luttinger liquid (LL) phase characterized by a gapless excitation spectrum. At the upper critical field  $H = H_{c2}$ , there is another QPT to the fully polarized ferromagnetic (FM) state. The magnetization data exhibit universal scaling behaviour in the vicinity of  $H_{c1}$  and  $H_{c2}$ , consistent with theoretical predictions [7, 8, 9, 10]. In the gapless regime  $H_{c1} < H < H_{c2}$ , the ladder Hamiltonian can be mapped onto an XXZ chain Hamiltonian the thermodynamic properties of which can be calculated exactly using the Bethe Ansatz (BA) [7, 8, 9, 10]. The theoretically computed magnetization versus magnetic field curve is in excellent agreement with the experimental data. QPTs can be observed in the organic ladder compounds as the magnitudes of the critical fields are experimentally accessible.

In recent years, QPTs have been extensively studied in spin systems using well-known quantum information theoretic measures. A number of entanglement measures have been identified which develop special features close to the quantum critical point [13, 14, 15, 16, 17, 18, 19]. It has been shown [16] that, in general, a first order QPT linked to a discontinuity in the first derivative of the ground state energy, is signalled by a discontinuity in a bipartite entanglement measure whereas a discontinuity or a divergence in the first derivative of the entanglement measure marks a second-order phase transition characterized by a discontinuity/divergence in the second derivative of the ground state energy. Another measure which provides a signature of QPTs is that of ground state fidelity [20, 21]. The utility of the measure and a related measure, fidelity susceptibility, has been explored in a number of studies [22, 23, 24, 25, 26, 27, 28]. Fidelity, a concept borrowed from quantum information theory, is defined as the overlap modulus between ground states corresponding to slightly different Hamiltonian parameters. The fidelity typically drops in an abrupt manner at a critical point indicating a dramatic change in the nature of the ground state wave function. This is accompanied by a divergence of the fidelity susceptibility. In these approaches, the fidelity measure involves global ground states. Recently, the concept reduced fidelity (RF) (also called partial state fidelity) has been developed, which relates to the fidelity of a subsystem [25, 29, 30, 31, 32, 33], along with the associated notion of reduced fidelity susceptibility (RFS). Using the RF and RFS measures, QPTs have been studied in spin models like the Lipkin-Meshkov-Glick model [30, 31], the transverse field Ising model in 1d [32] and the spin- $\frac{1}{2}$  dimerized Heisenberg chains [33]. In this paper, we use some well-known bipartite entanglement measures, which include one-site entanglement, two-site entanglement and concurrence, for the study of QPTs in the  $S = \frac{1}{2}$  two-leg AFM Heisenberg ladder (Fig. 1) described by the Hamiltonian given in Eq. (1). We show that the entanglement measures develop characteristic features close to the quantum critical point  $H = H_{c2}$  but not at the critical point  $H = H_{c1}$ . We next show that the measures based on the RF and RFS signal the occurrence of QPTs at both the critical points  $H = H_{c1}$  and  $H_{c2}$ .

## II. ENTANGLEMENT AND FIDELITY MEASURES PROBING QPTS

We first define the various entanglement and fidelity measures which provide the basis of our calculations. The single-site von Neumann entropy, a measure of the entanglement of a single spin with the rest of the system, is given by

$$S(i) = -\text{Tr} \rho(i) \log_2 \rho(i) \quad (2)$$

where  $\rho(i)$  is the single-site reduced density matrix [14, 19]. The two-site entanglement  $S(i, j)$  is a measure of the entanglement between two separate spins, at sites  $i$  and  $j$ , and the rest of the spins

[18, 19]. Let  $\rho(i, j)$  be the reduced density matrix for the two spins, obtained from the full density matrix by tracing out the spins other than the ones at sites  $i$  and  $j$ . The two-site entanglement is given by the von Neumann entropy

$$S(i, j) = -\text{Tr} \rho(i, j) \log_2 \rho(i, j) \quad (3)$$

In a translationally invariant system,  $S$  depends only on the distance  $n = |j - i|$ . A knowledge of the two-site reduced density matrix enables one to calculate concurrence, a measure of entanglement between two spins at sites  $i$  and  $j$  [34, 35]. Let  $\rho(i, j)$  be defined as a matrix in the standard basis  $\{|\uparrow\uparrow\rangle, |\uparrow\downarrow\rangle, |\downarrow\uparrow\rangle, |\downarrow\downarrow\rangle\}$ . One can define the spin-reversed density matrix as  $\tilde{\rho} = (\sigma_y \otimes \sigma_y) \rho^* (\sigma_y \otimes \sigma_y)$ , where  $\sigma_y$  is the Pauli matrix. The concurrence  $C$  is given by  $C = \max\{\lambda_1 - \lambda_2 - \lambda_3 - \lambda_4, 0\}$  where  $\lambda_i$ 's are square roots of the eigenvalues of the matrix  $\rho \tilde{\rho}$  in descending order.  $C = 0$  implies an unentangled state whereas  $C = 1$  corresponds to maximum entanglement.

The fidelity  $F$  is given by the modulus of the overlap of normalized ground state wave functions  $|\psi_0(\lambda)\rangle$  and  $|\psi_0(\lambda + \delta\lambda)\rangle$  for closely spaced Hamiltonian parameter values  $\lambda$  and  $\lambda + \delta\lambda$  [20, 21, 22].

$$F(\lambda, \lambda + \delta\lambda) = |\langle \psi_0(\lambda) | \psi_0(\lambda + \delta\lambda) \rangle| \quad (4)$$

Eq. (4) gives a definition of the global fidelity. The reduced fidelity (RF) [29, 30, 31, 32, 33] refers to a subsystem and is defined to be the overlap between the reduced density matrices  $\rho \equiv \rho(h)$  and  $\tilde{\rho} \equiv \rho(h + \delta)$  of the ground states  $|\phi_0(h)\rangle$  and  $|\phi_0(h + \delta)\rangle$ ,  $h$  and  $h + \delta$  being two closely spaced Hamiltonian parameter values. The RF is

$$F_R(h, h + \delta) = \text{Tr} \sqrt{\rho^{\frac{1}{2}} \tilde{\rho} \rho^{\frac{1}{2}}} \quad (5)$$

We now compute the different entanglement and fidelity measures for the ladder Hamiltonian given in Eq. (1). The external magnetic field  $H$  serves as the Hamiltonian parameter. One notes that the z-component,  $S_{tot}^z = \sum_{j=1}^L (S_{1,j}^z + S_{2,j}^z)$ , of the total spin is a conserved quantity. Using this fact, the Hamiltonian is diagonalized for different values of  $L$  with the help of the numerical diagonalization package TITPACK [36]. We take  $J_{\perp} = 13 K$  and  $J_{\parallel} = 1.15 K$  which are the approximate values of the rung and intrachain exchange couplings in the AFM compound  $(5IAP)2CuBr_4 \cdot 2H_2O$  [10]. We determine the ground state as well as the three lowest excited state energies for different values of  $H$  with  $L$  ranging from  $L = 2$  to  $L = 16$ . Using the data, we examine the variation of the fidelity  $F(H, H + \delta)$  (Eq. (4)) with increasing magnetic field strength  $H$  and  $\delta = .001$ . We observe sharp drops in  $F(H, H + \delta)$  at  $H_{C1}^L = \Delta_L$  (inset of Fig. 2), where  $\Delta_L$  is the spin gap, i.e., the difference in the energies of the first excited and ground states. A polynomial fitting of the  $\Delta_L$  versus  $\frac{1}{L}$  data points yields  $\Delta_L \approx 11.8416 + .9739(\frac{1}{L}) + .6621(\frac{1}{L})^2$ . In the thermodynamic limit  $L \rightarrow \infty$ , the critical field is thus  $H_{c1} = \Delta_{\infty} \approx 11.8416$ . In the case of the strong coupling ladder ( $J_{\perp} \gg J_{\parallel}$ ), the critical field  $H_{c1} \simeq J_{\perp} - J_{\parallel}$  to the first order in perturbation theory [37]. The fully polarized FM ground state ( $H > H_{c2}$ ) becomes unstable when the lowest energy of the spin waves falls below the energy of the polarized state. The magnitude of  $H_{c2}$  can be calculated exactly as  $H_{c2} = J_{\perp} + 2 J_{\parallel}$ . The estimates of  $H_{c1}$  and  $H_{c2}$  are in close agreement with the experimental results [2, 7, 37]. The numerical diagonalization data reproduces the exact value of  $H_{c2}$  in the thermodynamic limit. We further obtain the variation of the magnetization  $m(H)$  and its first derivative  $\frac{dm}{dH}$  with  $H$  in the thermodynamic limit adopting the extrapolation procedures outlined in [38]. The magnetization  $m(H)$  is the average magnetization per site and because of translational invariance  $m(H) = \langle S_i^z \rangle$ . At  $T = 0$ , the expectation value is calculated in the ground

state. The inset of Fig. (3) shows that the derivative  $\frac{dm}{dH}$  tends to diverge as  $H \rightarrow H_{c1}$  and  $H_{c2}$ . This is consistent with the existence of a square root singularity in  $m(H)$  in the vicinity of the quantum critical points  $H_{c1}$  and  $H_{c2}$  [7, 37]. Since second order QPTs occur at the critical fields  $H_{c1}$  and  $H_{c2}$ , the first derivatives of the entanglement measures,  $S(i)$ ,  $S(i, j)$  and  $C$ , with respect to the tuning parameter  $H$  may exhibit a discontinuity or a divergence as the critical points are approached [16]. We compute the various first derivatives to ascertain that this feature of critical point transitions holds true in the case of the spin ladder.

The single-site reduced density matrix  $\rho(i)$  can be written in terms of the spin expectation value  $\langle S_i^z \rangle$  as [31]

$$\rho(i) = \begin{pmatrix} \frac{1}{2} + \langle S_i^z \rangle & 0 \\ 0 & \frac{1}{2} - \langle S_i^z \rangle \end{pmatrix} \quad (6)$$

in the  $|\uparrow\rangle, |\downarrow\rangle$  basis. From Eq. (2),

$$S(i) = - \sum_i \lambda_i \log_2 \lambda_i \quad (7)$$

where the  $\lambda_i$  's are the two diagonal elements of  $\rho(i)$ . Fig. 3 shows the variation of  $\frac{dS(i)}{dH}$  with  $H$ . It is observed that unlike  $\frac{dm}{dH}$ ,  $\frac{dS(i)}{dH}$  tends to diverge only near  $H_{c2}$ , while it approaches a finite value close to  $H_{c1}$ . The values of  $H_{c1}$  and  $H_{c2}$  are  $H_{c1} = 11.8416 K$  and  $H_{c2} = 15.3 K$  as obtained from numerical diagonalization data. The strongly coupled ladder model in high magnetic field can be mapped onto a 1d  $XXZ$  AFM Heisenberg chain with an effective Hamiltonian [37, 39]

$$\mathcal{H}_{eff} = J_{||} \sum_{j=1}^L [\tilde{S}_j^x \tilde{S}_{j+1}^x + \tilde{S}_j^y \tilde{S}_{j+1}^y + \frac{1}{2} \tilde{S}_j^z \tilde{S}_{j+1}^z] - \tilde{H} \sum_{j=1}^L \tilde{S}_j^z \quad (8)$$

where  $\tilde{H} = H - J_{\perp} - \frac{J_{||}}{2}$  is an effective magnetic field and  $\tilde{S}_j^{\alpha}$  's ( $\alpha = x, y, z$ ) are pseudo spin- $\frac{1}{2}$  operators which can be expressed in terms of the original spin operators. There are several exact results known for the  $XXZ$  spin- $\frac{1}{2}$  chain in a magnetic field [40, 41]. In particular, the zero temperature magnetization  $m(H)$  close to the quantum critical points is given by the expressions (we use the symbol  $H$  instead of  $\tilde{H}$ )

$$m(H) \sim \frac{\sqrt{2}}{\pi} \sqrt{(H - H_{c1})/J_{||}}, \quad H > H_{c1} \quad (9)$$

$$m(H) \sim 1 - \frac{\sqrt{2}}{\pi} \sqrt{(H_{c2} - H)/J_{||}}, \quad H < H_{c2} \quad (10)$$

Similar expressions are obtained in the case of an integrable spin ladder model with the help of the thermodynamic BA [7]. Using the analytic expressions of  $m(H)$  in Eqs. (9) and (10), the first derivative of single-site von Neumann entropy with respect to magnetic field  $H$ ,  $\frac{dS(i)}{dH}$ , can be calculated analytically from Eqs. (2) and (6). Again, the derivative diverges near  $H_{c2}$  (Fig. 4) but not as the quantum critical point  $H_{c1}$  is approached, consistent with numerical results. The values of  $H_{c1}$  and  $H_{c2}$  are  $H_{c1} = J_{\perp} - J_{||} = 11.85 K$  and  $H_{c2} = J_{\perp} + 2 J_{||} = 15.3 K$ . The estimate of  $H_{c1}$  is from first-order perturbation theory.

The correlation functions of the  $S=\frac{1}{2}$   $XXZ$  chain in a magnetic field are known [42] in the gapless phase  $H_{c1} < H < H_{c2}$ . In terms of the original spin operators, these are given by

$$\langle S_1^z(r) S_1^z(0) \rangle = \frac{m^2}{4} + \frac{1}{r^2} + \cos(2\pi mr) \left( \frac{1}{r} \right)^{2K} \quad (11)$$

$$\langle S_1^+(r) S_1^-(0) \rangle = \cos[\pi(1-2m)r] \left( \frac{1}{r} \right)^{\frac{2K+1}{2K}} + \cos(\pi r) \left( \frac{1}{r} \right)^{\frac{1}{2K}} \quad (12)$$

where  $K$  is the LL exponent. For simplicity, we have dropped some prefactors (constants) in the terms appearing in Eqs (11) and (12). The expressions for the correlation functions are utilized to study the variation of the two-site entanglement  $S(i, j)$  and concurrence  $C_{i,i+1}$  with respect to the magnetic field. These quantities can be computed from the two-site reduced density matrix  $\rho(i, j)$  which, in terms of the spin expectation values and correlation functions, is given by [43]

$$\rho(i, j) = \begin{pmatrix} \frac{1}{4} + \langle S_i^z \rangle + \langle S_i^z S_j^z \rangle & 0 & 0 & 0 \\ 0 & \frac{1}{4} - \langle S_i^z S_j^z \rangle & \langle S_i^x S_j^x \rangle + \langle S_i^y S_j^y \rangle & 0 \\ 0 & \langle S_i^x S_j^x \rangle + \langle S_i^y S_j^y \rangle & \frac{1}{4} - \langle S_i^z S_j^z \rangle & 0 \\ 0 & 0 & 0 & \frac{1}{4} - \langle S_i^z \rangle + \langle S_i^z S_j^z \rangle \end{pmatrix} \quad (13)$$

$S(i, j)$  is given by

$$S(i, j) = - \sum_i \epsilon_i \log_2 \epsilon_i \quad (14)$$

where  $\epsilon_i$ 's are the eigenvalues of  $\rho(i, j)$ . Using equation (9), (10), (11) (12) and (13), the first derivative of  $S(i, j)$  with respect to  $H$  is calculated near both the critical points (Fig. 5). The derivative diverges near  $H_{c2}$  but approaches a finite value close to  $H_{c1}$ . The n.n. concurrence can be written as [14, 34, 35]

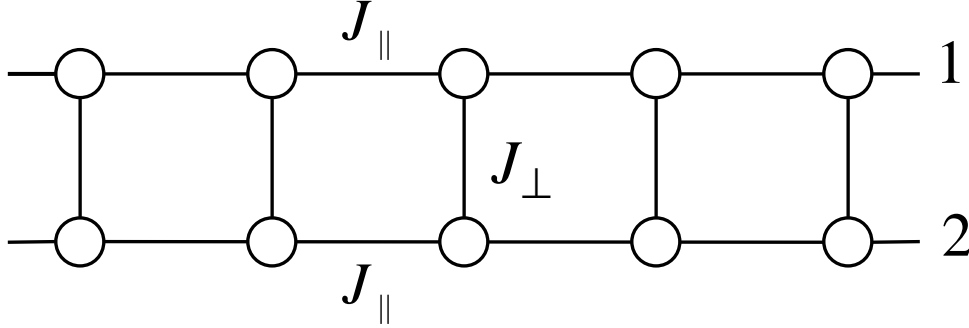
$$C_{i,i+1} = 2 \text{Max}[0, |\rho_{23}(i, i+1)| - \sqrt{\rho_{11}(i, i+1)\rho_{44}(i, i+1)}] \quad (15)$$

Fig. 6 shows the derivative of  $C_{i,i+1}$  with respect to  $H$  versus  $H$ . The derivative, as in the case of one-site and two-site entanglement measures, diverges as  $H \rightarrow H_{c2}$  but has a finite value as  $H \rightarrow H_{c1}$ .

Lastly, we probe the existence of special features, if any, near the QCPs exhibited by the one-site RF [25, 29, 30, 31, 32, 33] defined in Eq. (5). The reduced fidelity susceptibility (RFS) is defined to be

$$\chi_R(H) = \lim_{\delta \rightarrow 0} \frac{-2 \ln \mathcal{F}_R(H, H + \delta)}{\delta^2} \quad (16)$$

Figs. (7) and (8) show that the RF  $\mathcal{F}_R(H, H + \delta)$  drops sharply at the quantum critical points (*insets*) and the associated RFS,  $\chi_R(H)$ , blows up as both the quantum critical points are approached. This result is in contrast with what is observed in the case of entanglement measures, where a special feature develops only in the vicinity of the critical point  $H_{c2}$ . The calculations of the RF and the RFS are possible because they involve only local measures. A calculation of the global fidelity would not have been possible lacking a knowledge of the true many body ground state.



**FIG. 1:** A two-chain ladder with rung and intra-chain nearest-neighbour exchange couplings of strengths  $J_{\perp}$  and  $J_{\parallel}$  respectively. The indices **1** and **2** label the two chains of the ladder.

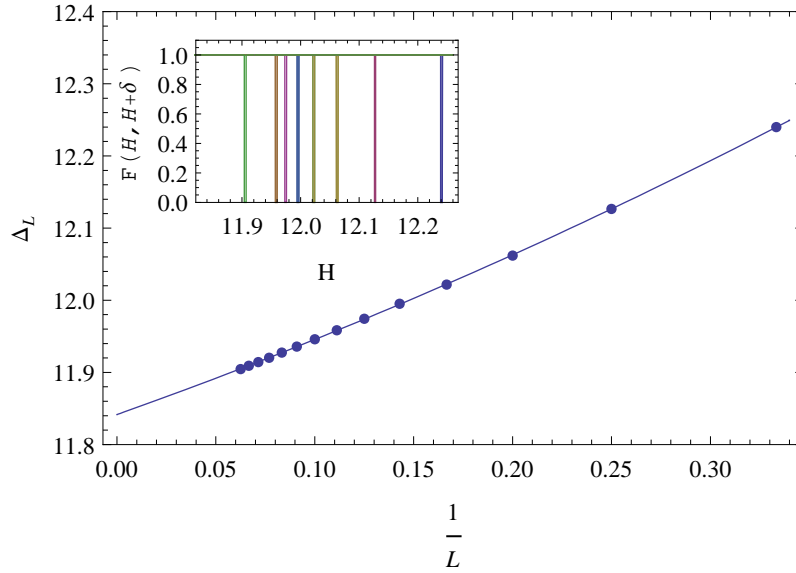


**FIG. 2:** Plot of  $\Delta_L$ , the spin gap, versus  $\frac{1}{L}$  from numerical diagonalization data of the ladder Hamiltonian (Eq. (1)),  $L$  being the number of rungs in the ladder. (*inset*) ground state fidelity versus magnetic field  $H$  for  $L = 3, 4, \dots, 16$ .

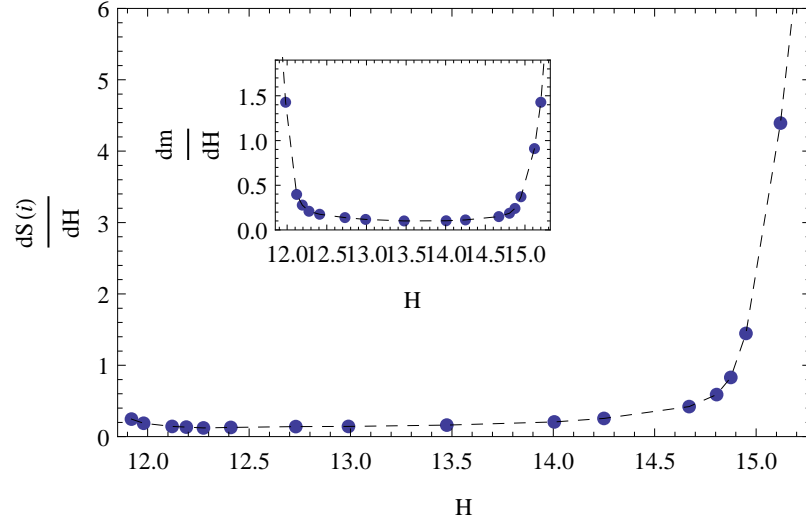


**FIG. 3:** Plot of  $\frac{dS(i)}{dH}$  versus  $H$  (using numerical diagonalization data); (*inset*) variation of  $\frac{dm}{dH}$  with  $H$ .

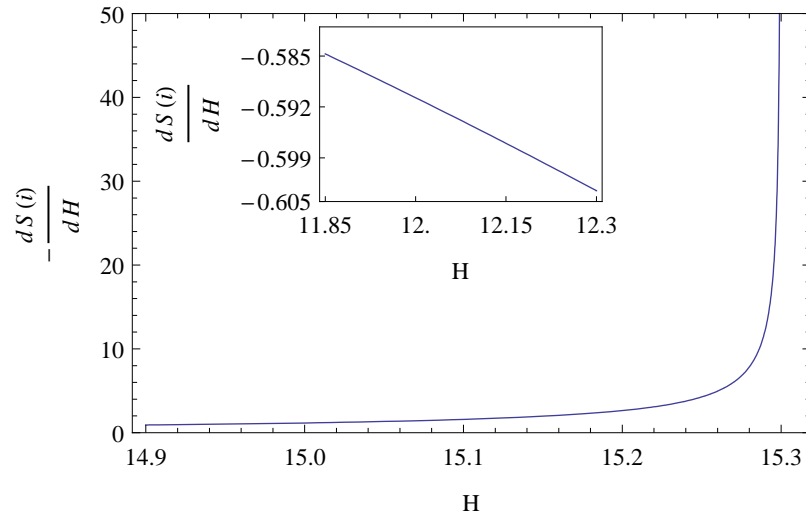


**FIG. 4:** Plot of  $\frac{dS(i)}{dH}$  versus  $H$  near  $H = H_{c2}$ ; (*inset*) plot of  $\frac{dS(i)}{dH}$  versus  $H$  near  $H_{c1}$ .



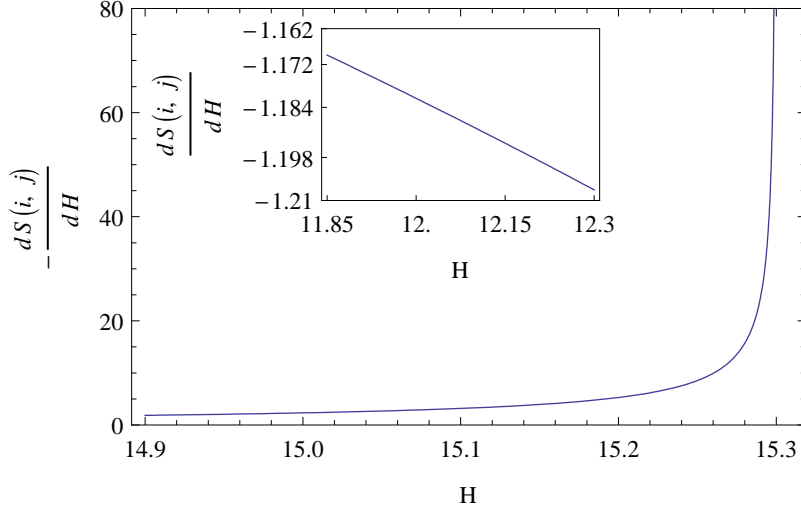


**FIG. 5:** Plot of  $\frac{dS(i,j)}{dH}$  versus  $H$  near  $H = H_{c2}$ ; (*inset*) plot of  $\frac{dS(i,j)}{dH}$  versus  $H$  near  $H_{c1}$ .

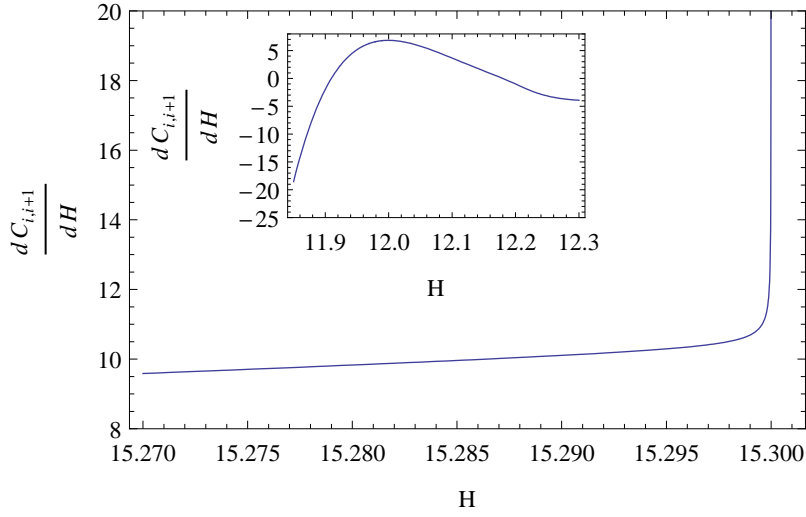


**FIG. 6:** Plot of  $\frac{dC_{i,i+1}}{dH}$  versus  $H$  near  $H = H_{c2}$ ; (*inset*) plot of  $\frac{dC_{i,i+1}}{dH}$  versus  $H$  near  $H_{c1}$ .

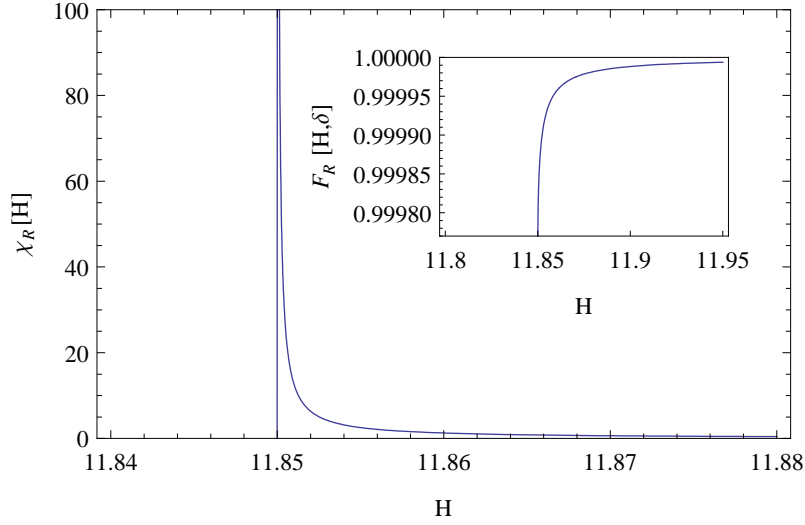


**FIG. 7:** Plot of RFS  $\chi_R(H)$  versus  $H$  near  $H = H_{c1}$ ; (*inset*) plot of RF  $F_R(H, H + \delta)$  versus  $H$  near  $H = H_{c1}$ .

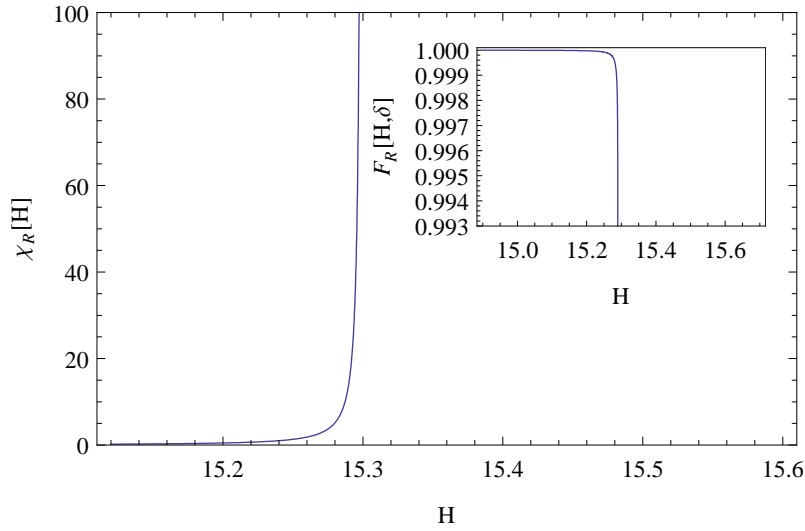


**FIG. 8:** Plot of RFS  $\chi_R(H)$  versus  $H$  near  $H = H_{c2}$ ; (*inset*) plot of RF  $F_R(H, H + \delta)$  versus  $H$  near  $H = H_{c2}$ .

## IV. DISCUSSIONS

In this paper, we consider a spin- $\frac{1}{2}$ , two-chain AFM ladder in an external magnetic field. The ladder system is known to exhibit QPTs at two critical values,  $H_{c1}$  and  $H_{c2}$ , of the magnetic field. The ladder has a rich quantum phase diagram with a gapless LL phase separating two gapped phases. Both the spin-disordered state ( $0 < H < H_{c1}$ ) and the fully polarized FM state ( $H > H_{c2}$ ) constitute gapped phases. Using a bosonization technique, it has been shown [44] that the spin gaps vanish at the critical points and the spin-spin correlation functions become long-ranged. As suggested in [16, 17, 18], a second order QPT is characterized by a discontinuous/divergent first derivative of an entanglement measure with respect to the tuning parameter. Our computations of the first derivatives of the entanglement measures  $S(i)$ ,  $S(i, j)$  and  $C_{i,i+1}$  show that these quantities diverge only as  $H \rightarrow H_{c2}$  but remain finite as the other critical point  $H_{c1}$  is approached. As discussed in [16], the first derivatives of one or more elements of the reduced density matrix  $\rho(i, j)$  with respect to the tuning parameter are expected to diverge at the critical points. From Eqs. (11)-(13), one can verify that this is the case as  $H \rightarrow H_{c1}$  and  $H_{c2}$  with the divergent contributions coming from  $\rho_{11}(i, j)$  and  $\rho_{44}(i, j)$ . The theorem in [16] regarding the discontinuity/divergence of the first derivative of an entanglement measure at a critical point links the behaviour to that of the first derivative of one or more elements of  $\rho(i, j)$ . This is so provided a set of conditions is satisfied. We find that one of these conditions (condition (b)) is violated in the case of the two-chain ladder as  $H \rightarrow H_{c1}$ . This is easily illustrated for the entanglement measure  $C_{i,i+1}$  (Eq. (15)). The first derivative  $\frac{dC_{i,i+1}}{dH}$  involves terms containing the factor  $m(H)\frac{dm(H)}{dH}$  which leads to a cancellation of singularities as  $H \rightarrow H_{c1}$  (see Eq. (9)). This is contrary to condition (b) in [16] so that the theorem is no longer valid. The cancellation of singularities does not occur as  $H \rightarrow H_{c2}$  (see Eq. (10)) so that  $\frac{dC_{i,i+1}}{dH}$  signals the occurrence of a QPT. In the case of the single-site entanglement,  $S(i)$ , similar arguments show that the cancellation of the singularity occurs as  $H \rightarrow H_{c1}$ . The square root singularities in magnetization (Eqs. (9) and (10)) are generic to other AFM systems with spin gap like the spin-1 chain in a magnetic field [44, 45, 46]. Thus, the behaviour reported in this paper may be a general feature of a class of gapped 1d AFM systems. As shown in our paper, the measures RF and RFS yield appropriate signatures as both the critical points  $H_{c1}$  and  $H_{c2}$  are approached and thus appear to be better indicators of QPTs in the case of systems which violate one or more conditions of the theorem in [16].

## ACKNOWLEDGMENT

A. T. is supported by the Council of Scientific and Industrial Research, India, under Grant No. 9/15 (306)/ 2004-EMR-I. The authors are grateful to H. Nishimori for sending the full TITPACK program package used in the present study.

## References

- [1] E. Dagotto and T. M. Rice, Science 271, 618 (1996).
- [2] E. Dagotto, Rep. Prog. Phys. 62, 1525 (1999).
- [3] E. Dagotto, Rev. Mod. Phys. 66, 763 - 840 (1994)

- [4] E. Dagotto, J. Riera and D. Scalapino, Phys. Rev. B 45, 5744 (1992).
- [5] S. Gopalan, T. M. Rice and M. Sigrist, Phys. Rev. B 49, 8901 (1994).
- [6] I. Bose and S. Gayen, Phys. Rev. B 48, 10653 (1993).
- [7] M. T. Batchelor, X. W. Guan, N. Oelkers and Z. Tsuboi, Adv. Phys. 56, 465 (2007).
- [8] G. Chaboussant, P.A. Crowell, L. P. Lévy, O. Piovesana, A. Madouri and D. Mailly, Phys. Rev. B, 55 3046 (1997).
- [9] B.C. Watson et al., Phys. Rev. Lett., 86 5168 (2001).
- [10] C.P. Landee, M.M. Turnbull, C. Galeriu, J. Giantsidis and F.M. Woodward, Phys. Rev. B 63 100402 (2001).
- [11] S. Sachdev, Science 288, 475 (2000)
- [12] S. Sachdev, Quantum Phase Transitions, Cambridge University Press, Cambridge, 1999.
- [13] A. Osterloh, L. Amico, G. Falci, and R. Fazio, Nature (London) 416, 608 (2002).
- [14] T. J. Osborne and M. A. Nielsen, Phys. Rev. A 66, 032110, (2002).
- [15] G. Vidal, J. I. Latorre, E. Rico, and A. Kitaev, Phys. Rev. Lett. 90, 227902 (2003).
- [16] L.-A. Wu, M. S. Sarandy and D. A. Lidar, Phys. Rev. Lett. 93, 250404 (2004).
- [17] T. R. Oliveira, G. Rigolin, M. C. de Oliveira and E. Miranda, Phys. Rev. Lett. 97, 170401 (2001).
- [18] H.-D. Chen, J. Phys. A 40, 10215 (2007).
- [19] A. Tribedi and I. Bose, Phys. Rev. A 75, 042304 (2007).
- [20] H. T. Quan, Z. Song, X. F. Liu, P. Zanardi, and C. P. Sun, Phys. Rev. Lett. 96, 140604 (2006).
- [21] P. Zanardi and N. Paunković, Phys. Rev. E 74, 031123 (2006).
- [22] M. Cozzini, R. Ionicioiu and P. Zanardi, Phys. Rev. B 76, 104420 (2007).
- [23] M. Cozzini, P. Giorda and P. Zanardi, Phys. Rev. B 75, 014439 (2007).
- [24] P. Buonsante and A. Vezzani, Phys. Rev. Lett. 98, 110601 (2007).
- [25] H.-Q. Zhou, e-print arXiv:0704.2945.
- [26] P. Zanardi, M. Cozzini and P. Giorda, J. Stat. Mech.: Theory Exp. (2007), L02002.
- [27] P. Zanardi, H. T. Quan, X. Wang and C. P. Sun, Phys. Rev. A 75, 032109 (2007).
- [28] S. Chen, L. Wang, S. J. Gu and Y. Wang, Phys. Rev. E 76, 061108 (2007).
- [29] N. Paunković, P. D. Sacramento, P. Nogueira, V. R. Vieira and V. K. Dugaev, Phys. Rev. A 77, 052302 (2008).

- [30] H.-M. Kwok, C.-S. Ho and S.- J. Gu, Phys. Rev. A 78, 062302 (2008).
- [31] J. Ma, L. Xu, H. Xiong and X. Wang, arXiv:0805.4062.
- [32] J. Ma, L. Xu and X. Wang, arXiv:0808.1816.
- [33] H.-N. Xiong, J. Ma, Z. Sun and X. Wang, arXiv:0808.1817.
- [34] K. M. O'Connor and W. K. Wootters, Phys. Rev. A 63, 052302 (2001); W. K. Wootters, Phys. Rev. Lett. 80, 2245 (1998).
- [35] M. C. Arnesen, S. Bose and V. Vedral, Phys. Rev. Lett 87, 017901 (2001); D. Gunlycke, V. M. Kendon, V. Vedral and S. Bose, Phys. Rev. A 64, 042302 (2001).
- [36] H. Nishimori, AIP Conf. Proc. 248, 269-278 (1992).
- [37] G. Chaboussant et al., Eur. Phys. J. B 6, 167 (1998).
- [38] T. Sakai and M. Takahashi, Phys. Rev. B 43, 13383 (1991).
- [39] F. Mila, Eur. Phys. J. B 6, 201 (1998).
- [40] C. N. Yang and C. P. Yang, Phys. Rev. 150, 327 (1966).
- [41] F. D. M. Haldane, Phys. Rev. Lett. 47, 1840 (1981).
- [42] T. Giamarchi and A. M. Tsvelik, Phys. Rev. B 59, 11398 (1999).
- [43] U. Glaser, H. Büttner and H. Fehske, Phys. Rev. A 68, 032318 (2003).
- [44] R. Chitra and T. Giamarchi, Phys. Rev. B 55, 5816 (1997).
- [45] H. J. Schulz, Phys. Rev. B 22, 5274 (1980).
- [46] I. Affleck, Phys. Rev. B 43, 3215 (1991).